Electronic Supplementary Information

Room Temperature Doping of Ln^{3+} in Perovskite Nanoparticles: A Halide Exchange Mediated Cation Exchange Approach

Gouranga H. Debnath,[1] Brian P. Bloom,[1] Susheng Tan[2,3] and David H. Waldeck[1,3,*]

[1]Department of Chemistry, University of Pittsburgh, Pittsburgh, Pennsylvania 15260, United States

[2]Department of Electrical and Computer Engineering, University of Pittsburgh, Pittsburgh, Pennsylvania 15261, United States

[3]Petersen Institute of NanoScience and Engineering, University of Pittsburgh, Pittsburgh, Pennsylvania 15261, United States

E-mail: dave@pitt.edu

* To whom correspondence should be addressed.

Table of Contents

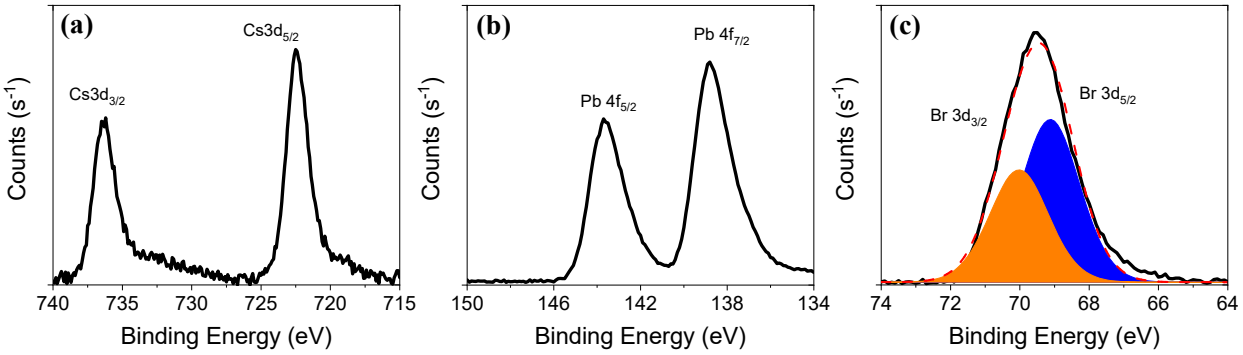

Figure S1. XPS spectra of the $CsPbBr_3$ NPs are shown. The Br3d spectra, panel (c), was fit to a doublet corresponding to the Br $3d_{5/2}$ (blue) and Br $3d_{3/2}$ (orange) orbitals. The red dashed line is an envelope for the multicomponent fitting.

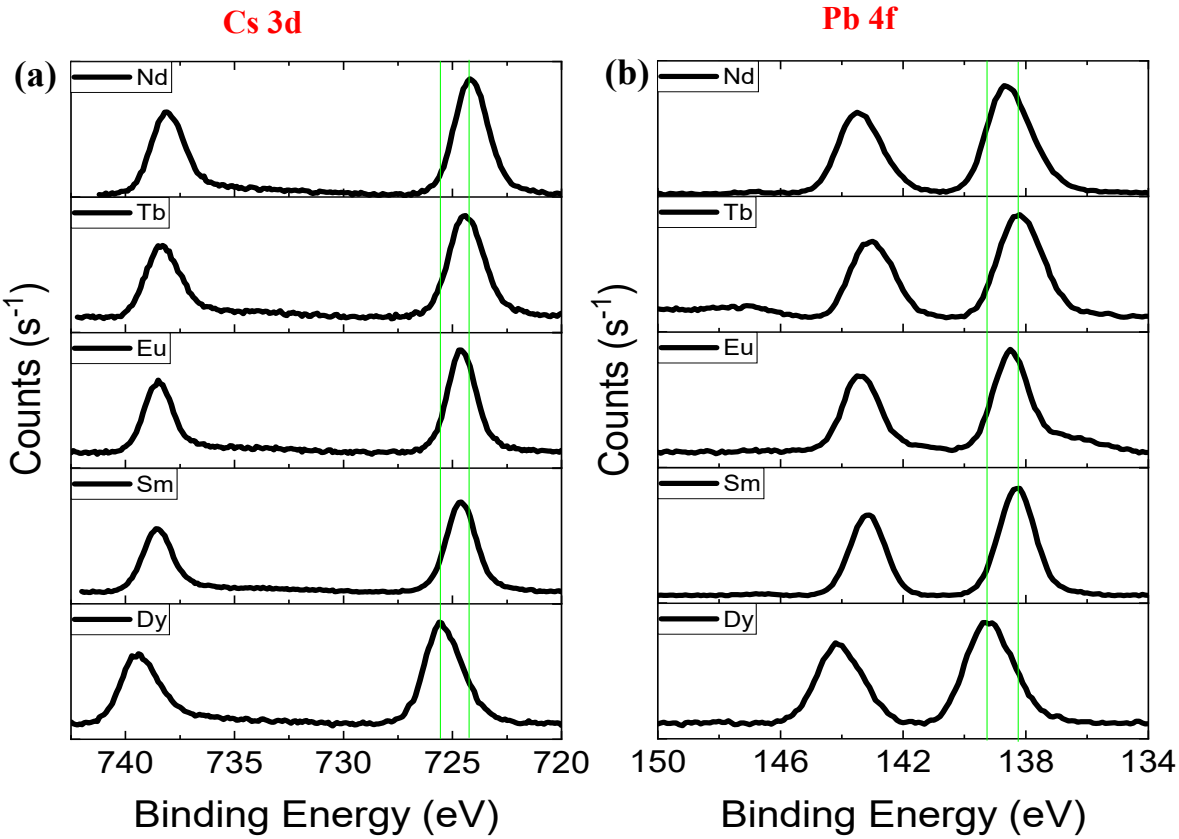

Figure S2. (a) Cs3d and (b) Pb4f XPS spectra of the $CsPbBr_3/LnCl_3$ NPs [Ln = Nd, Tb, Eu, Sm, and Dy] are shown. The green lines show the relative shift, upper and lower limit, in binding energy of the orbitals for the different Ln dopants.

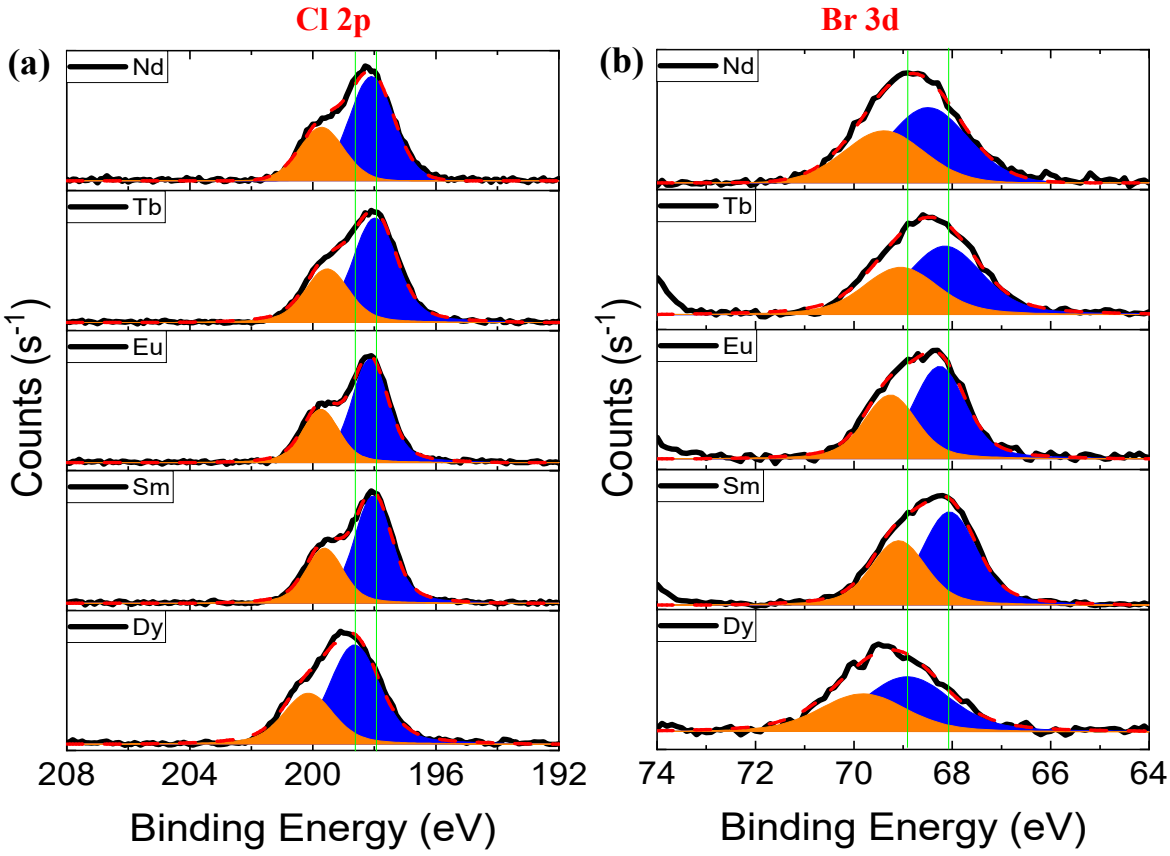

Figure S3. (a) Cl2p and (b) Br3d XPS spectra of the $CsPbBr_3/LnCl_3$ NPs [Ln = Nd, Tb, Eu, Sm, and Dy]. Each spectrum is fit to a doublet corresponding to the Cl $2p_{3/2}$ (blue) and Cl $2p_{1/2}$ (orange) orbitals in panel (a) and Br $3d_{5/2}$ (blue) and Br $3d_{3/2}$ (orange) orbitals in panel (b). The red dashed line is an envelope for the multicomponent fitting. The green lines show the relative shift, upper and lower limit, in binding energy of the Cl $2p_{3/2}$ and Br $3d_{5/2}$ orbitals for the different Ln dopants.

Table S1. Atomic percentages of the different elements present in $CsPbBr_3$, and $CsPbBr_3/LnCl_3$ NPs are shown.

System	Cs (%)	Pb (%)	Br (%)	Cl (%)	Ln (%)
$CsPbBr_3$	18	19.6	62.4	0	0
$CsPbBr_3/NdCl_3$	12.6	10.9	12.9	61.5	2.1
$CsPbBr_3/SmCl_3$	12.7	9.6	18.4	53.8	5.5
$CsPbBr_3/EuCl_3$	11.2	6.4	10.4	67.0	5.0
$CsPbBr_3/TbCl_3$	9.6	6.6	13.0	65.0	5.8
$CsPbBr_3/DyCl_3$	13.8	5.0	7.7	65.2	8.3

The propensity for enhanced Ln^{3+} incorporation in the NPs as a function of increasing Ln^{3+} atomic number can be explained in terms of decreasing ionic radius of the Ln^{3+} (e.g. ionic radii of Nd^{3+} and Dy^{3+} are 112.3pm and 105.2pm respectively.)

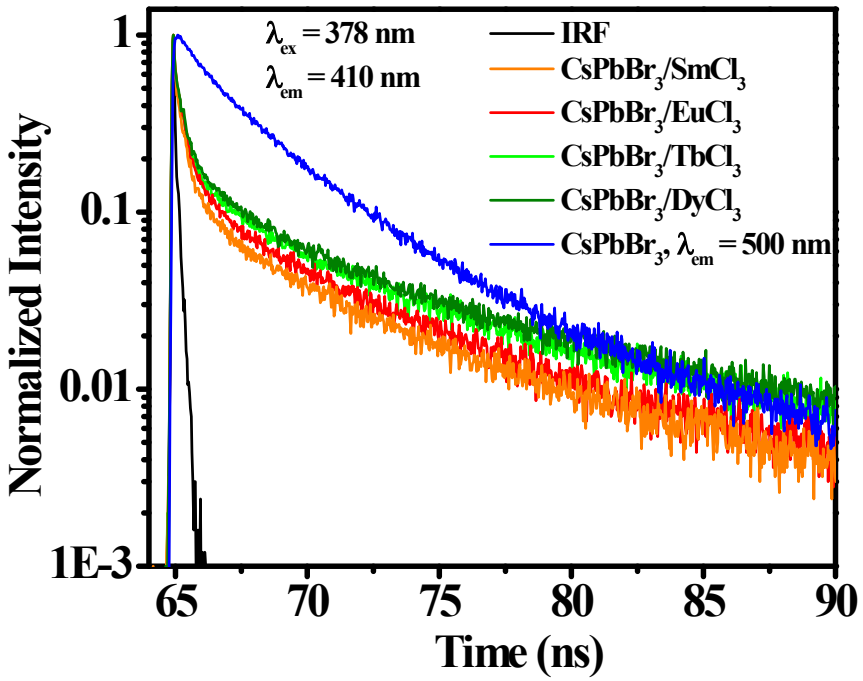

Figure S4. Emission decay profiles of the $CsPbBr_3$ and $CsPbBr_3/LnCl_3$ NPs [Ln = Sm, Eu, Tb, and Dy] in toluene are shown.

Table S2. Lifetime Parameters of the different NPs studied.[1]

System ($CsPbBr_3/LnCl_3$)	a_1	τ_1 (ns)	a_2	τ_2 (ns)	a_3	τ_3 (ns)	$\langle\tau\rangle$ (ns)
$CsPbBr_3$	0.52 ± 0.01	1.0 ± 0.09	0.45 ± 0.01	3.33 ± 0.16	0.03 ± 0.002	11.30 ± 0.28	2.35 ± 0.08
Ln = Sm	0.95 ± 0.02	0.30 ± 0.01	0.04 ± 0.01	2.85 ± 0.07	0.01 ± 0.002	10.32 ± 0.32	0.49 ± 0.03
Ln = Eu	0.96 ± 0.005	0.31 ± 0.03	0.03 ± 0.001	2.71 ± 0.41	0.01 ± 0.001	10.0 ± 0.74	0.50 ± 0.03
Ln = Tb	0.93 ± 0.04	0.33 ± 0.01	0.06 ± 0.02	3.10 ± 0.14	0.01 ± 0.001	11.75 ± 0.07	0.60 ± 0.06
Ln = Dy	0.94 ± 0.03	0.35 ± 0.02	0.05 ± 0.01	3.08 ± 0.04	0.01 ± 0.001	12.2 ± 0.4	0.60 ± 0.04

[1]The decays are fitted to a multiexponential model using the equation $I(t) = \Sigma a_i \exp(-t/\tau)$, where $\Sigma a_i = 1$.
[2]$\langle\tau\rangle = a_1\tau_1 + a_2\tau_2 + a_3\tau_3$ with τ_1, τ_2, and τ_3 being the three lifetime components having relative amplitudes a_1, a_2, and a_3 respectively. $\chi^2 \leq 1.2$.

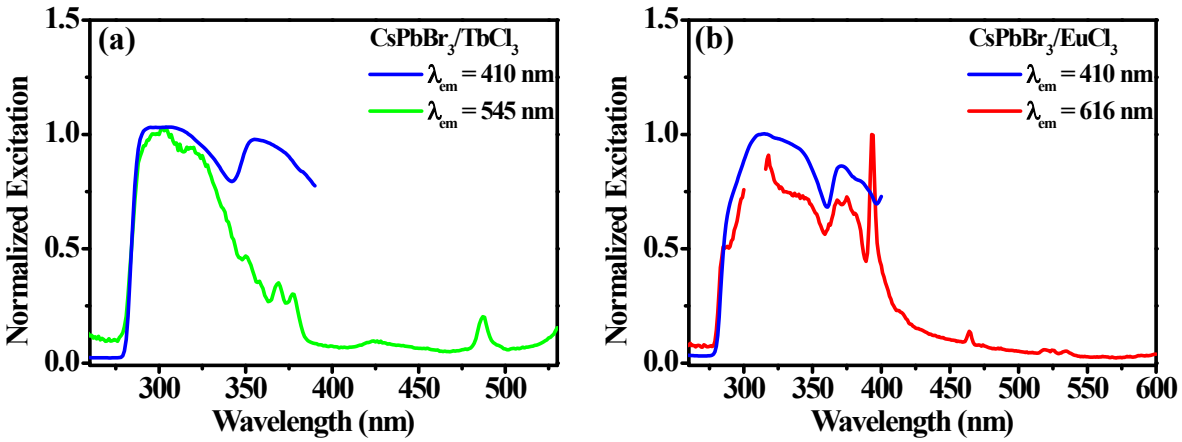

Figure S5. Steady-state photoluminescence excitation spectra of (a) $CsPbBr_3/TbCl_3$ and (b) $CsPbBr_3/EuCl_3$ NPs in toluene are shown.

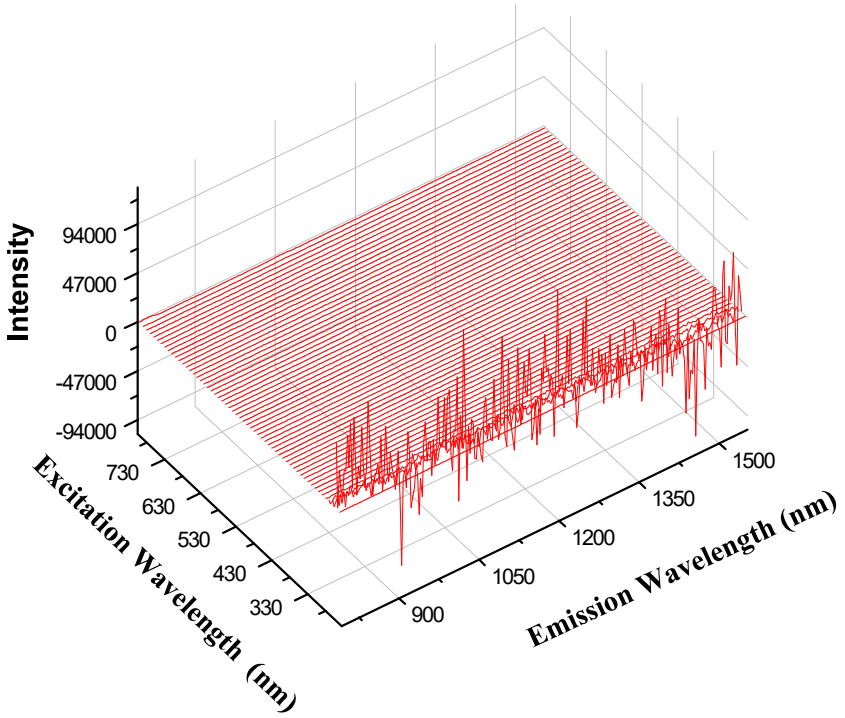

Figure S6. 2D photoluminescence excitation profile of the $CsPbBr_3/NdCl_3$ NPs in toluene is shown.

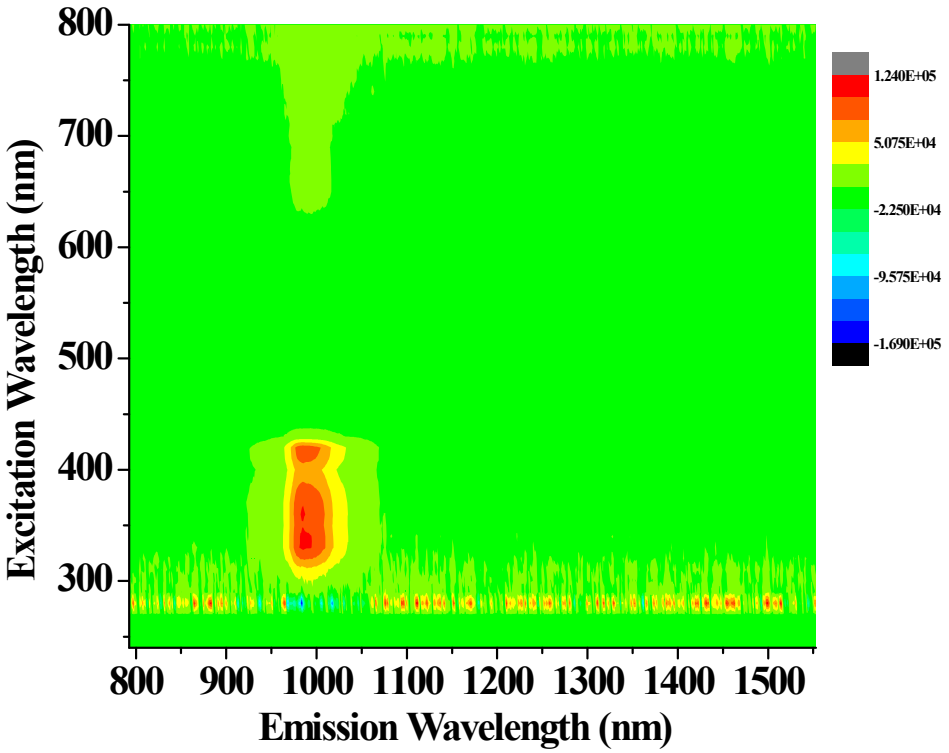

Figure S7. Photoluminescence excitation map of the $CsPbBr_3/YbCl_3$ NPs in toluene is shown.

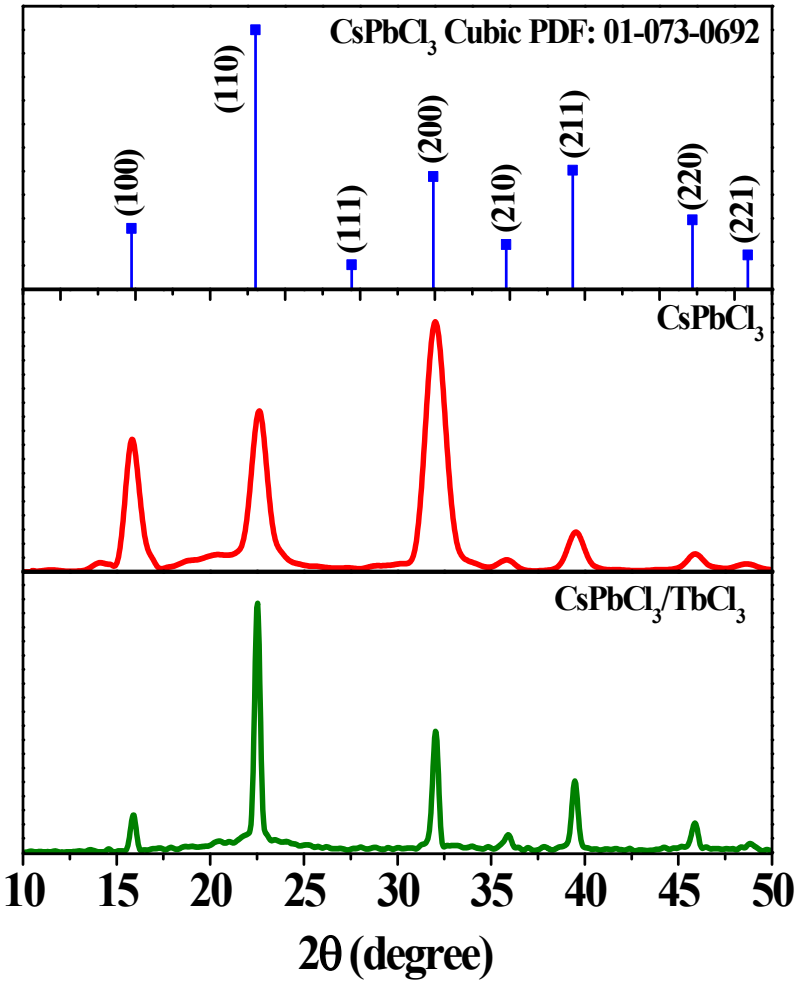

Figure S8. XRD patterns of $CsPbCl_3$ and $CsPbCl_3/TbCl_3$ NPs are shown.

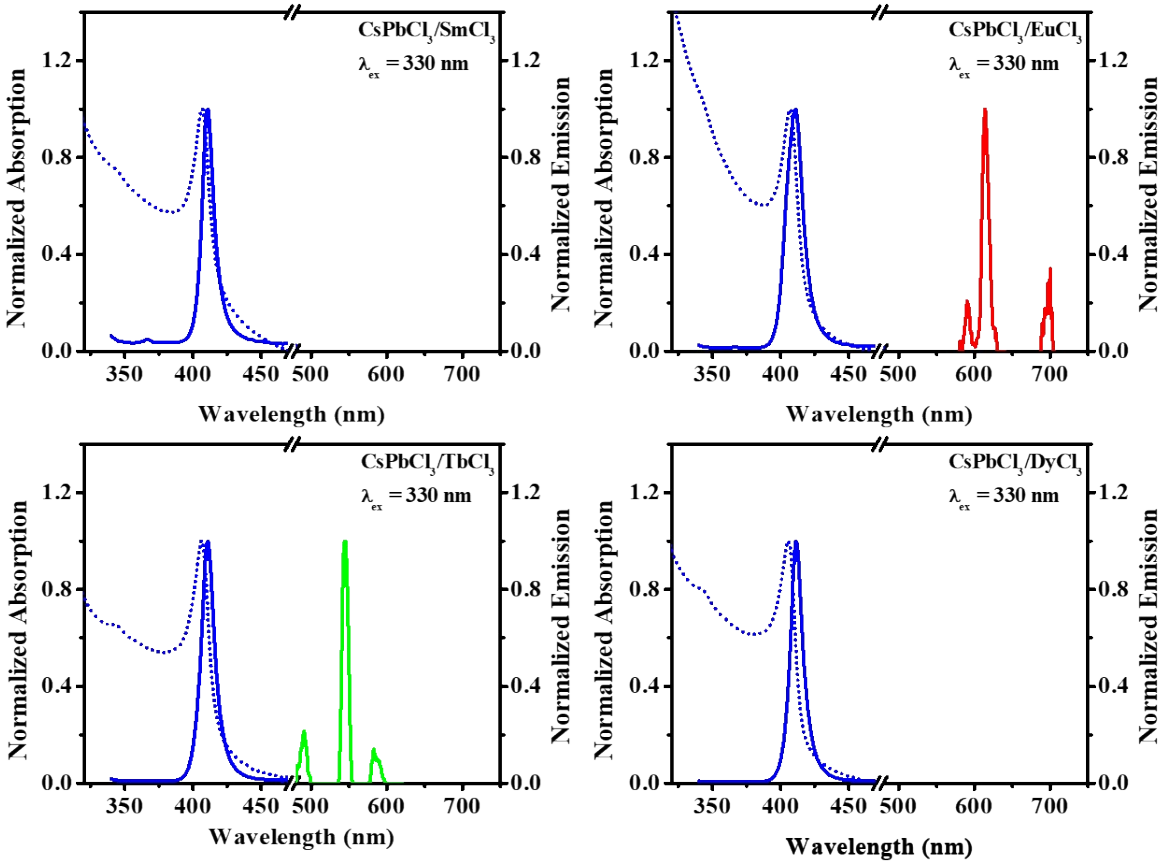

Figure S9. Steady-state photoluminescence emission spectra of the $CsPbCl_3/LnCl_3$ NPs [Ln = Sm, Eu, Tb, and Dy] in toluene are shown.

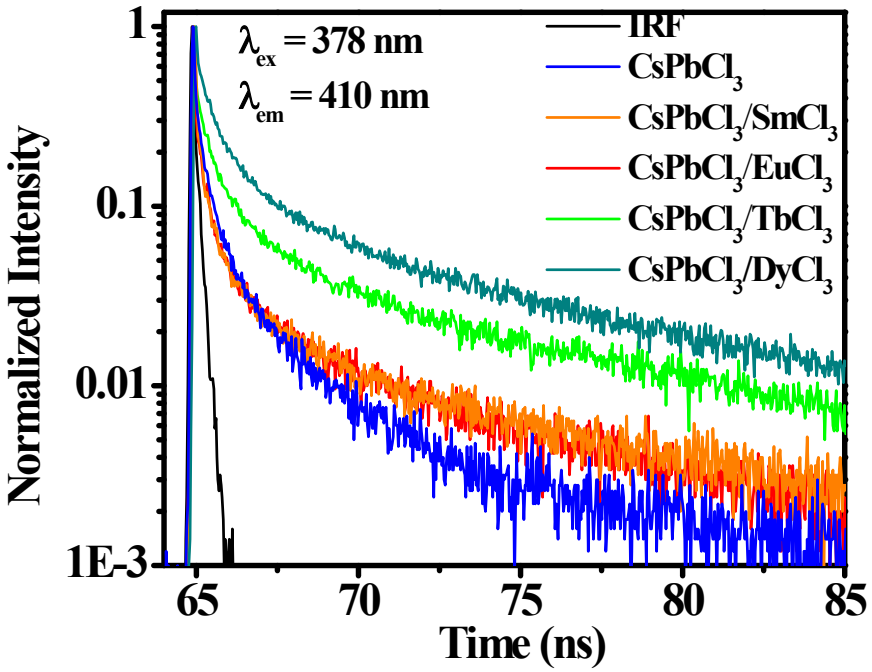

Figure S10. Emission decay profiles of the $CsPbCl_3$ and $CsPbCl_3/LnCl_3$ NPs [Ln = Sm, Eu, Tb, and Dy] are shown. The NPs were dispersed in toluene.

Table S3. Lifetime Parameters of the different NPs studied.[1]

System ($CsPbCl_3/LnCl_3$)	a_1	τ_1	a_2	τ_2	a_3	τ_3	$\langle\tau\rangle$ (ns)
Ln = Dy	0.87 ± 0.01	0.32 ± 0.02	0.1 ± 0.01	1.30 ± 0.15	0.03 ± 0.004	8.30 ± 0.20	0.63 ± 0.08
Ln = Sm	0.91 ± 0.02	0.18 ± 0.04	0.07 ± 0.02	1.10 ± 0.12	0.02 ± 0.002	7.65 ± 0.35	0.39 ± 0.01
Ln = Tb	0.87 ± 0.02	0.32 ± 0.02	0.1 ± 0.01	1.55 ± 0.21	0.03 ± 0.007	8.95 ± 0.35	0.74 ± 0.14
Ln = Eu	0.90 ± 0.04	0.19 ± 0.02	0.08 ±0.03	1.15 ± 0.07	0.02 ± 0.007	7.35 ± 0.35	0.43 ± 0.06
$CsPbCl_3$	0.86 ± 0.03	0.19 ± 0.04	0.12 ± 0.03	0.98 ± 0.08	0.02 ± 0.003	4.38 ± 0.02	0.37 ± 0.02

[1]The decays are fitted to a multiexponential model using the equation $I(t) = \Sigma a_i \exp(-t/\tau)$, where $\Sigma a_i = 1$.
[2]$\langle\tau\rangle = a_1\tau_1 + a_2\tau_2 + a_3\tau_3$ with τ_1, τ_2, and τ_3 being the three lifetime components having relative amplitudes a_1, a_2, and a_3 respectively. $\chi^2 \leq 1.2$.

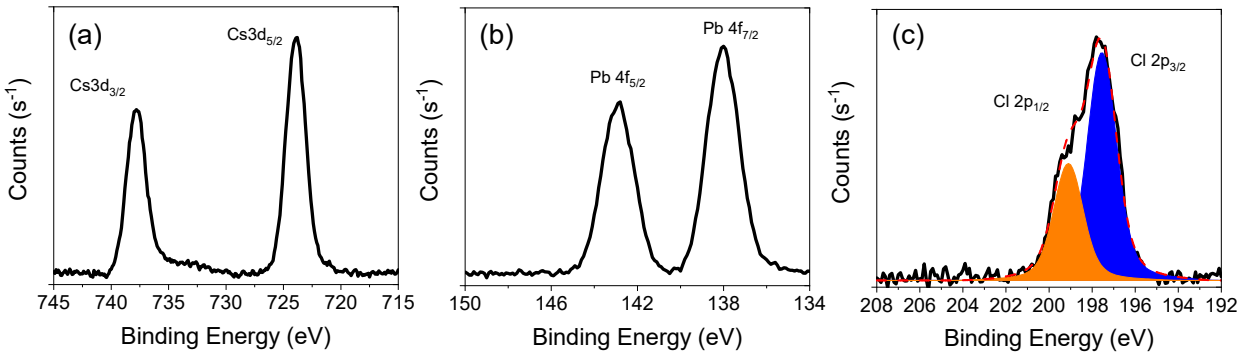

Figure S11. XPS spectra of the $CsPbCl_3$ NPs are shown. The Chlorine 2p spectrum is fit to a doublet corresponding to the Cl $2p_{3/2}$ (blue) and Cl $2p_{1/2}$ (orange) orbitals. The red dashed line is an envelope for the multicomponent fitting.

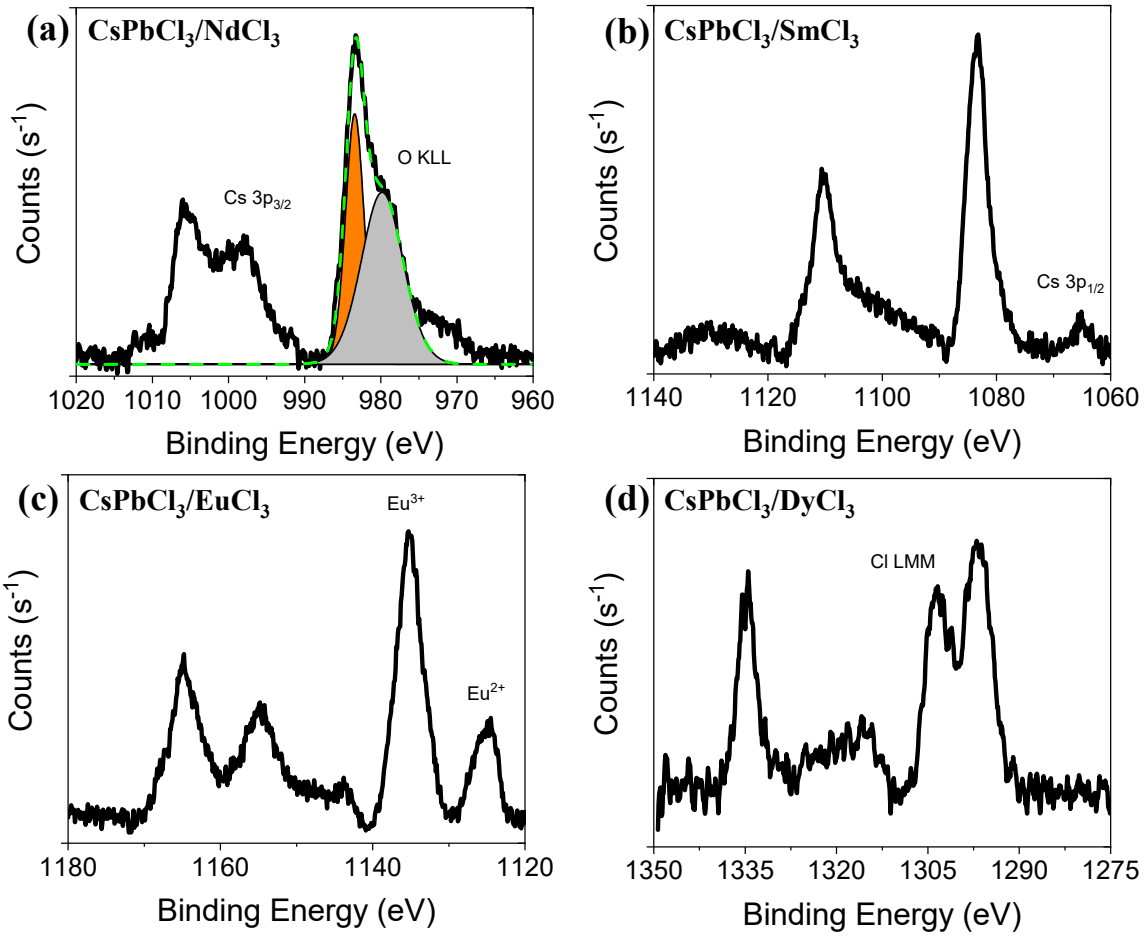

Figure S12. XPS spectra of $CsPbCl_3/LnCl_3$ NPs [Ln = Nd, Sm, Eu, and Dy] are shown. Panels (a) through (d) correspond to Nd3d, Sm3d, Eu3d, and Dy3d respectively. Signatures arising from peaks other than lanthanides are marked. For panel (a), the data were fit to a sum of peaks where the peak of interest is highlighted in orange and the green dashed line is an envelope for the multicomponent fitting.

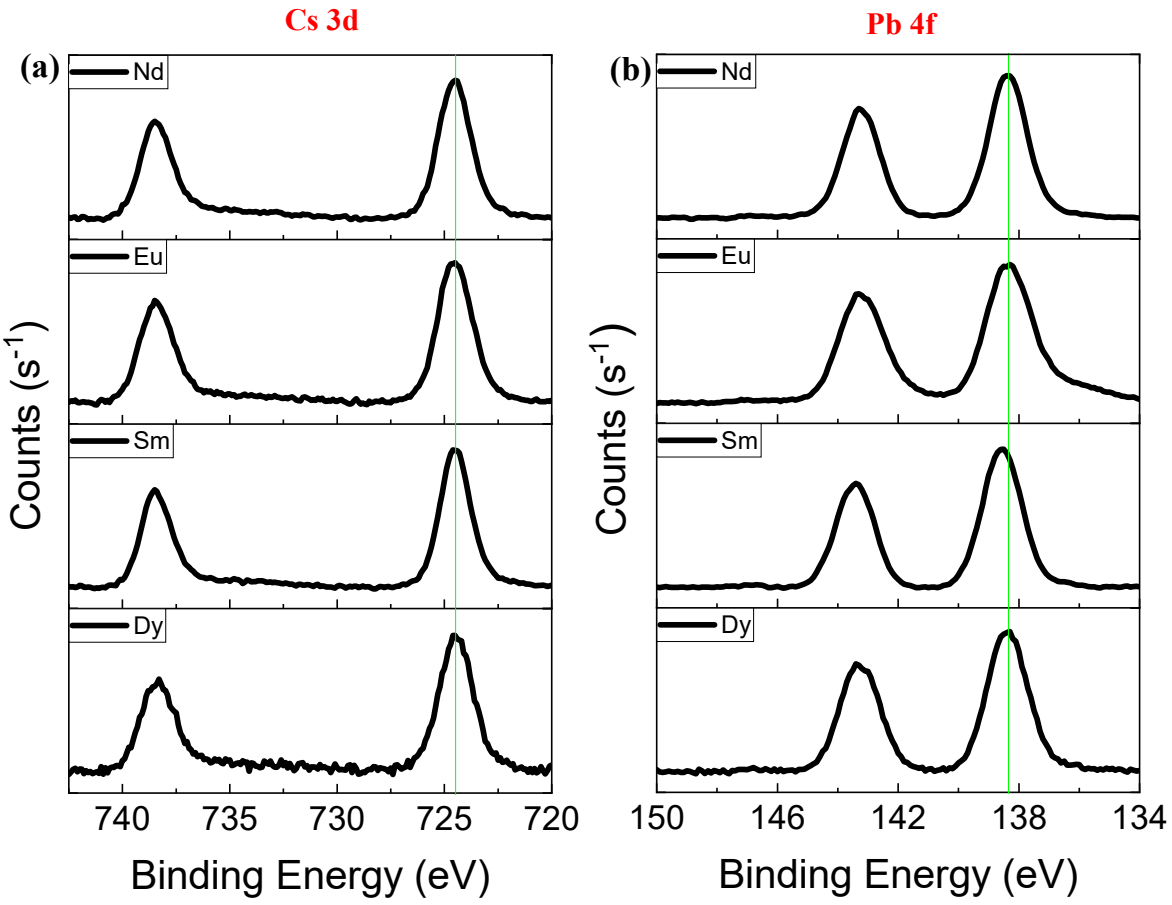

Figure S13. (a) Cs3d and (b) Pb4f XPS spectra of the $CsPbCl_3/LnCl_3$ NPs [Ln = Nd, Eu, Sm, and Dy] are shown. The green lines show the relative shift, upper and lower limit, in binding energy of the Cs $3d_{5/2}$ and Pb $4f_{7/2}$ orbitals for the different Ln dopants.

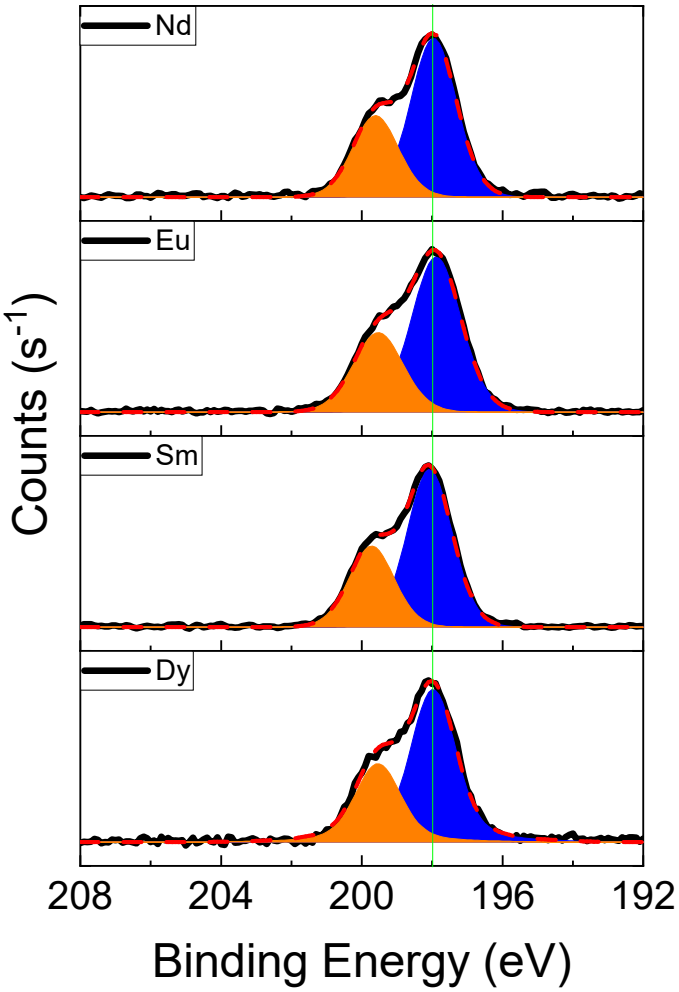

Figure S14. Cl2p XPS spectra of the $CsPbCl_3/LnCl_3$ NPs [Ln = Nd, Eu, Sm, and Dy]. The Chlorine 2p spectra are fit to a doublet corresponding to the Cl $2p_{3/2}$ (blue) and Cl $2p_{1/2}$ (orange) orbitals. The red dashed line is an envelope for the multicomponent fitting and the green line is a guide to the eye for the relative binding energy shift for each dopant

Table S4. Atomic percentages of the different elements present in $CsPbCl_3$, and $CsPbCl_3/LnCl_3$ NPs are shown. The error in calculation of the atomic percentage is ~10% of the value reported in the table.

System	Cs (%)	Pb (%)	Cl (%)	Ln (%)
$CsPbCl_3$	23.0	16	61	0
$CsPbCl_3/NdCl_3$	9.7	13.7	74.7	1.9
$CsPbCl_3/SmCl_3$	10.9	10.9	72.9	5.3
$CsPbCl_3/EuCl_3$	11.9	11.3	71.4	5.4
$CsPbCl_3/DyCl_3$	8.5	10.6	77.8	3.1

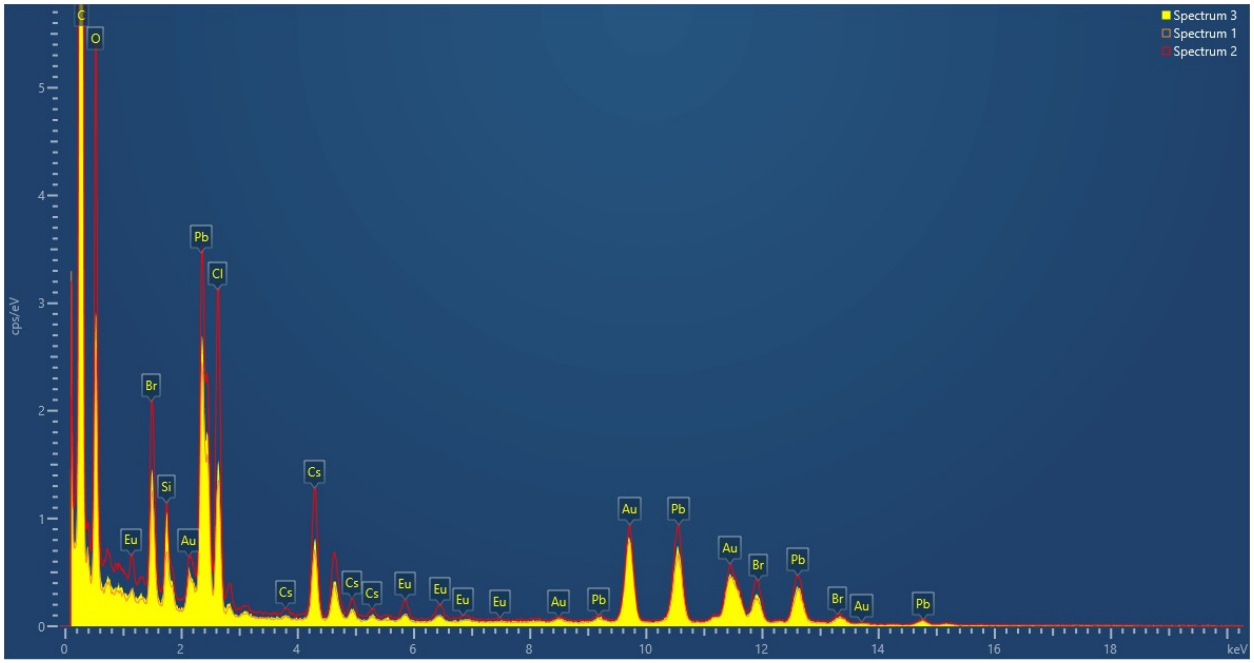

Figure S15. EDX spectra of the $CsPbBr_3/EuCl_3$ NPs are shown.

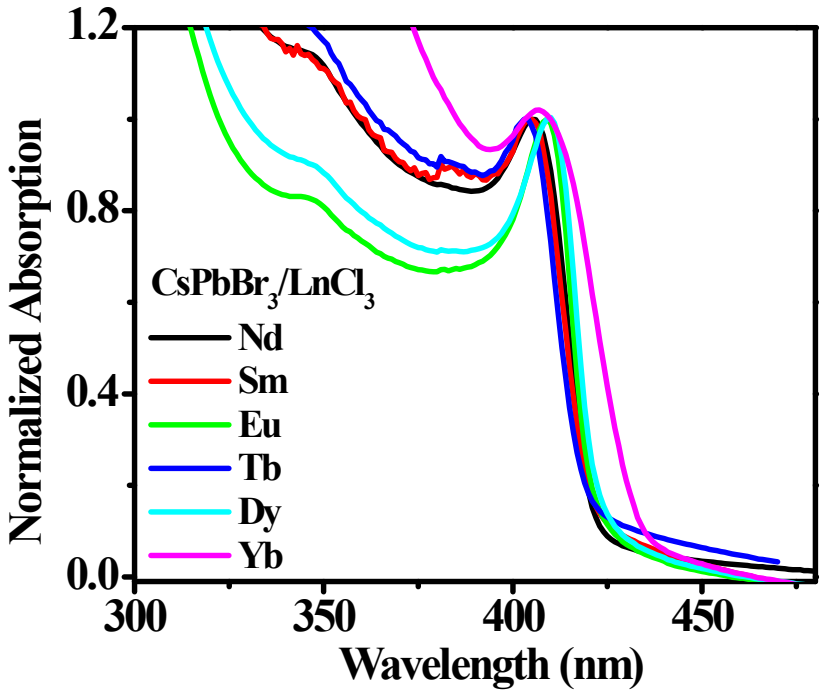

Figure S16. Normalized absorption spectra of the $CsPbBr_3/LnCl_3$ NPs in toluene are shown.

A Förster Resonance Energy Transfer (FRET) Mediated Sensitization Mechanism:

The rate constant for non-radiative energy transfer, k_{ET}, in a Förster energy transfer mechanism is given by

$$k_{ET} = \frac{1}{\tau_F}(R_0/R)^6 \tag{i}$$

where

$$R_0{}^6 = \frac{9000(ln10)\Phi_D 2}{128\pi^5 n^4 N \quad 3} J_F \; ; \; [J_F = \frac{\int_0^\infty F_D(\bar{\nu})\varepsilon_A(\bar{\nu})\bar{\nu}^{-4} d\bar{\nu}}{\int_0^\infty F_D(\bar{\nu}) d\bar{\nu}}] \tag{ii}$$

Here τ_F is the average lifetime of the donor chromophore; R_0, the critical distance at which the rate of energy transfer equals the reciprocal of donor emission lifetime; and R is the distance between donor and acceptor. The critical distance R_0 is given by (ii) in which Φ_D is the donor emission quantum yield in absence of acceptor; *n* is the refractive index of the medium; N is Avogadro's number; $F_D(\bar{\nu})$ is the donor chromophore's emission spectrum (in wavenumbers) in the absence of acceptor Ln^{3+}; and $\varepsilon_A(\bar{\nu})$ is the molar extinction coefficient of Ln^{3+} acceptor on a wavenumber scale.

For a FRET based sensitization to be operating, the spectral overlap between the donor emission and the acceptor absorption is a prerequisite. Note the lack of such a possibility in Figure S17, which shows the $CsPbCl_3$ NP emission and the $YbCl_3$ absorption spectra; thereby proving that FRET is not a good predictor to rationalize Yb^{3+} sensitization in $CsPbCl_3$ NPs.

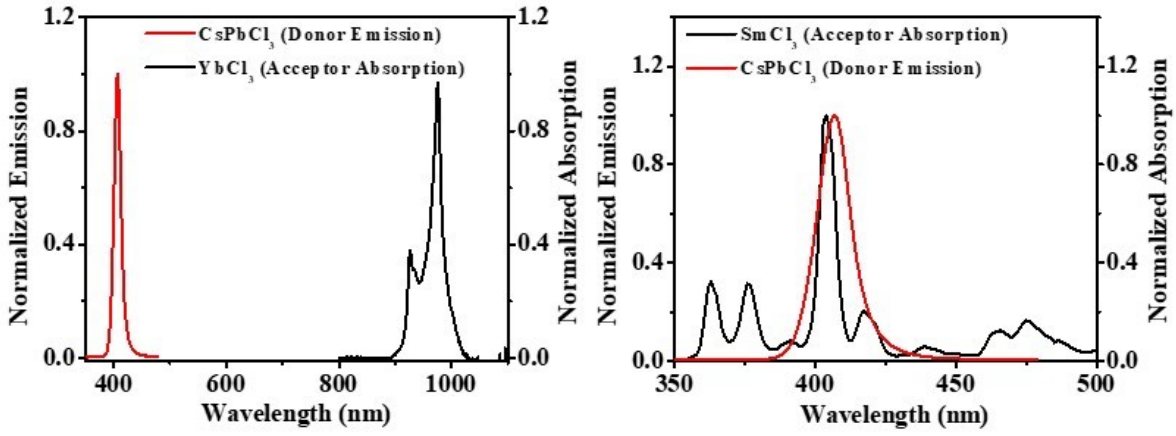

Figure S17. (Left Panel) Normalized emission spectra of $CsPbCl_3$ NPs (in toluene) and absorption spectra of anhydrous $YbCl_3$ (in anhydrous DMF) are shown. Note the lack of any significant donor-acceptor spectral overlap, which implies that a Förster resonance energy transfer-based mechanism cannot be used to rationalize Yb^{3+} sensitization in $CsPbCl_3$ in NPs. (Right Panel) Normalized emission spectra of $CsPbCl_3$ NPs (in toluene) and absorption spectra of anhydrous $SmCl_3$ (in

anhydrous DMF) are shown. Note that the spectral overlap should indicate significant Sm^{3+} sensitization, which is in contrast to the trend observed.